

# Calculation of Temperature-Dependent Thermal Expansion Coefficient of Metal Crystals Based on Anharmonic Correlated Debye Model

Tong Sy Tien<sup>\*</sup>, Nguyen Thi Minh Thuy, Vu Thi Kim Lien, Nguyen Thi Ngoc Anh,  
Do Ngọc Bích, Le Quang Thanh

Department of Basic Sciences, University of Fire Prevention and Fighting, Hanoi, Vietnam

Received 09 May 2022; received in revised form 07 August 2022; accepted 17 August 2022

DOI: <https://doi.org/10.46604/aiti.2023.10034>

## Abstract

This study aims to calculate the anharmonic thermal expansion (TE) coefficient of metal crystals in the temperature dependence. The calculation model is derived from the anharmonic correlated Debye (ACD) model that is developed using the many-body perturbation approach and correlated Debye model based on the anharmonic effective potential. This potential has taken into account the influence on the absorbing and backscattering atoms of all their nearest neighbors in the crystal lattice. The numerical results for the crystalline zinc (Zn) and crystalline copper (Cu) are in agreement with those obtained by the other theoretical model and experiments at several temperatures. The analytical results show that the ACD model is useful and efficient in analyzing the TE of coefficient of metal crystals.

**Keywords:** thermal expansion coefficient, metal crystals, anharmonic correlated Debye model

## 1. Introduction

In recent years, the anharmonic thermal expansion (TE) coefficient has been widely used to determine many dynamic properties of materials [1]. Like the compressibility and heat capacity, the TE coefficient is important because it is one of the independent thermodynamic properties which can be measured experimentally with high precision [2]. Accurate information on the TE coefficient in the temperature dependence is required for the metallurgical industry as well as in engineering physics [3]. The TE coefficient is often used to determine the matching between different metal components in the alloy [4]. A large difference in the TE coefficients between the metal components can lead to adverse deformation in the alloy when the temperature changes [5]. Moreover, the position of atoms and their interatomic distance always changes and are not stationary under the influence of thermal vibrations [6]. This influence causes thermal disorder and anharmonic effects in the crystal lattice, so the TE coefficient is sensitive to the temperature change and can be varied with increasing temperature [7].

In materials science, high precision measurements of lattice parameters using the X-ray method based on the development of the theory of the crystal structures have become increasingly important. Moreover, the accurate determination of lattice parameters enables one to investigate the TE coefficient of various crystalline substances, even if the weight of the substances available for measurement is only a few milligrams [2, 4].

Besides, the extended X-ray absorption fine structure (EXAFS) technique is a widely employed probe of the dynamical behaviors and structural parameters in disordered systems [8]. It is because EXAFS spectroscopy can contain information on local structures around X-ray absorbing atoms and gives interatomic distances and coordination numbers in crystal lattices [9].

---

<sup>\*</sup> Corresponding author. E-mail address: [tongsytien@yahoo.com](mailto:tongsytien@yahoo.com)

Tel.: +849-1-2439564; Fax: +849-8-1439564

This resulted in the EXAFS technique being developed and expanded greatly based on the rapid development of synchrotron radiation facilities worldwide [10]. In reality, thermal disorders can disturb the EXAFS oscillation [6, 9], so the TE coefficient is also sensitive to EXAFS oscillation under the influence of temperature.

Nowadays, metals and advances in manufacturing processes have brought us the industrial revolutions, so it becomes irreplaceable materials in the growth of human civilization. They are used extensively in manufacturing machines for industries, agriculture or farming, and automobiles, including road vehicles, railways, airplanes, rockets, etc. [2-4]. The TE of coefficient of metal crystals has also been investigated using the anharmonic correlated Einstein (ACE) model [11-12] and experiments [11-13]. Still, this model only uses a unique correlated Einstein frequency to describe the atomic vibrations, so it cannot mimic the acoustic phonon branches presenting in lattice crystals.

Recently, an anharmonic correlated Debye (ACD) model [14] can treat even the acoustic phonon branches presenting in lattice crystals because it describes the atomic vibrations using the frequencies varying from 0 to the correlated Debye frequency. It has also been efficiently used to investigate the anharmonic thermodynamic properties of many materials [9, 15-16]. Still, it has not yet been used to analyze the anharmonic TE coefficient of metal crystals. Therefore, the calculation and analysis of the temperature-dependent TE coefficient of metal crystals based on extending the ACD model will be a necessary addition to experimental data analysis in the advanced material technique.

## 2. Calculation of the Anharmonic TE Coefficient

Usually, the TE coefficient  $\alpha_T(T)$  characterizes the net thermal expansion (NTE) caused by thermal vibrations in the crystal lattice [17], as shown in Fig. 1.

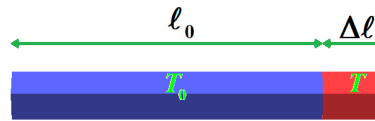


Fig. 1 Thermal expansion of metal with a change in temperature

The TE coefficient can be determined [11-12] by:

$$\alpha_T(T) = \frac{\Delta \ell}{\ell_0 \Delta T} \approx \frac{dr(T)}{r_0 dT} = \frac{d\sigma^{(1)}(T)}{r_0 dT} \quad (1)$$

where  $T$  is the absolute temperature,  $r(T)$  is the instantaneous distance between the backscattering and absorbing atoms,  $r_0$  is the equilibrium distance between the backscattering and absorbing atoms, and  $\sigma^{(1)}(T)$  is the first EXAFS cumulant and can be expressed in terms of the power moments of the radial pair distribution (RD) function [18-19]:

$$\sigma^{(1)}(T) = r(T) - r_0 \quad (2)$$

Normally, the Morse potential can validly determine the pair interaction (PI) potential of the crystals [20-21]. If this potential is expanded up to the third-order around its minimum position, it can be written as

$$\varphi(x) = D(e^{-2\alpha x} - 2e^{-\alpha x}) \cong -D + D\alpha^2 x^2 - D\alpha^3 x^3, \quad x = r(T) - r_0 \quad (3)$$

where  $D$  is the dissociation energy,  $\alpha$  is the width of the potential, and  $x$  is the deviation distance between the backscattering and absorbing atoms.

To determine the thermodynamic parameters of a system, it is necessary to specify its anharmonic effective (AE) potential and force constants [8, 22]. One considers a monatomic system with an AE potential (ignoring the constant contribution) is extended up to the third-order:

$$V_{eff}(x) = \frac{1}{2}k_{eff}x^2 - k_3x^3 \quad (4)$$

where  $k_{eff}$  is the effective force constant,  $k_3$  is the local force constant giving asymmetry of potential due to the inclusion of anharmonicity, and these force constants are considered in the temperature independence.

In the relative vibrations of absorbing Eq. (1) and backscattering Eq. (2) atoms, including the effect of correlation and taking into account only the nearest-neighbor interactions, the AE potential [23-24] is given using the PI potential, i.e.

$$V_{eff} = V(x) + \sum_{i=1,2} \sum_{j \neq 1,2} V(\varepsilon_i x \hat{R}_{12} \hat{R}_{ij}), \quad \varepsilon_i = \frac{\mu}{M_i} \quad (5)$$

where  $M_i$  ( $i = 1, 2$ ) is the mass of the  $i$ th atom and equals  $m$  in the monatomic crystals, respectively,  $\mu = M_1 M_2 / (M_1 + M_2)$  is the reduced mass of the absorber and backscatter,  $R_{ij}$  is a unit vector, the sum  $i$  is the over absorbers ( $i = 1$ ) and backscatters ( $i = 2$ ), the sum  $j$  is over the nearest neighbors, and.

The ACD model is derived from the dualism of an elementary particle in quantum theory and is perfected based on the correlated Debye model using the AE potential and many-body perturbation approach [9, 14]. It is often used effectively in treating monatomic systems with less complex phonon density of states and multiple acoustic phonons [15-16]. In this model, the atomic vibrations can be quantized and treated as a system consisting of many phonons, in which each atomic vibration corresponds to a wave that has a frequency  $\omega(q)$  and is described via the dispersion relation

$$\omega(q) = \omega_D \left| \sin\left(\frac{qa}{2}\right) \right|, \quad \omega_D = 2\sqrt{\frac{k_0}{m}}, \quad |q| \leq \frac{\pi}{a} \quad (6)$$

where  $q$  is the phonon wavenumber in the first Brillouin (FB) zone,  $a$  is the lattice constant, and  $\omega_D$  is the correlated Debye frequency and characterizes the atomic thermal vibrations.

The general expression of the first EXAFS cumulant in the ACD model was calculated in the temperature dependence by Hung et al. [14]. Still, these obtained expressions are not optimized yet because they still depend on the lattice constant  $a$ . In this investigation, the previous ACD model has been extended to calculate the temperature-dependent TE coefficient of metal crystals.

After using the general expression of the first EXAFS cumulant and converting from variable  $q$  to variable  $p$  in the formula  $p=qa/2$ , the temperature-dependent first cumulant of metal crystals are obtained as

$$\sigma^{(1)}(T) = \frac{3\hbar k_3}{\pi k_{eff}^2} \int_0^{\pi/2} \omega(p) \frac{1 + \exp[-\hbar\omega(p)/k_B T]}{1 - \exp[-\hbar\omega(p)/k_B T]} dp = \frac{3\hbar k_3}{\pi k_{eff}^2} \int_0^{\pi/2} \omega(p) \coth[\hbar\omega(p)/2k_B T] dp \quad (7)$$

Substituting this cumulant into Eq. (1) to calculate the temperature-dependent TE coefficient of metal crystals, it yields

$$\alpha_T(T) = \frac{3\hbar k_3}{\pi r_0 k_{eff}^2} d \left\{ \int_0^{\pi/2} \omega(p) \coth[\hbar\omega(p)/2k_B T] dp \right\} / dT \quad (8)$$

Using an approximation  $\exp\{-\hbar\omega(p)/k_B T\} \approx 0$ , the TE coefficient of metal crystals in the low-temperature (LT) limit ( $T \rightarrow 0$ ) can be calculated from Eq. (8), i.e.

$$\alpha_T(T) \approx \frac{2\pi k_B^2 k_3 T}{\hbar r_0 \omega_D k_{eff}^2} \quad (9)$$

Using an approximation  $\exp\{-\hbar\omega(p)/k_B T\} \approx 1 - \hbar\omega(p)/k_B T$ , the TE coefficient of metal crystals in the high-temperature (HT) limit ( $T \rightarrow \infty$ ) can be calculated from Eq. (8), that is

$$\alpha_T(T) = \frac{3k_3k_B}{r_0k_{eff}^2} \quad (10)$$

Thus, an extended ACD model has been perfected to efficiently calculate the temperature dependence of the TE coefficient of metal crystals. The obtained expressions using this model can satisfy all their fundamental properties in the temperature dependence. These expressions have also been optimized to not depend on the lattice constant  $a$  as in the previous ACD model [14-15].

### 3. Numerical Result and Discussion

In this section, the obtained expressions using the ACD model in Sec. 2 are applied to the numerical calculations of crystalline zinc (Zn) and crystalline copper (Cu) that have the hexagonal close-packed (HCP) and face-centered cubic (FCC) structures, respectively. Herein, the local force constants  $k_{eff}$  and  $k_3$ , the correlated Einstein frequency  $\omega_D$ , and the temperature-dependent first EXAFS cumulant  $\sigma^{(1)}(T)$  and TE coefficient  $\alpha_T(T)$  are the quantities to be performed in numerical calculations. These obtained numerical results are compared with those obtained using the ACE [11-12, 22-23, 25] and experiments [11-13, 22, 26-28]. From these obtained comparisons, the development and effectiveness of the ACD model are analyzed and discussed in investigating the temperature-dependent thermal expansion coefficient of metal crystals. The following is the presentation of these numerical results:

The AE potential of Zn and Cu can be calculated using Eq. (5) based on the Morse potential in Eq. (3) and the crystal structure properties of these metals. After ignoring the overall constant in the obtained result and comparing it with Eq. (4), the local force constants  $k_{eff}$  and  $k_3$  are deduced in the expressions of the Morse potential parameters  $D$  and  $\alpha$ , while the correlated Debye frequency  $\omega_D$  is calculated using Eq. (6) via the effective force constant  $k_{eff}$ .

The values of the local force constants  $k_{eff}$  and  $k_3$  and the correlated Debye frequency  $\omega_D$  of Zn and Cu are given in Table 1. Herein, the obtained results of the correlated Debye frequency  $\omega_D$  using the ACE [22, 25] are inferred from the correlated Einstein frequency  $\omega_E$  and related expression  $\omega_D = \sqrt{2}\omega_E$  [9, 23-24, 28]. Meanwhile, the obtained results using the experimental EXAFS data are derived from the measured Morse potential parameters and Eq. (6). It can be seen that the obtained results using the ACD model fit with those obtained using the ACE [22-23, 25] and experimental data [22, 27], especially for the correlated Debye frequency  $\omega_D$  and effective force constant  $k_{eff}$ .

Table 1 The thermodynamic parameters  $k_0$ ,  $k_3$ , and  $\omega_D$  of Zn and Cu obtained using the ACD and ACE models and experiments

Metal	Method	Mass	$D$ (eV)	$\alpha$ ( $\text{\AA}^{-1}$ )	$r_0$ ( $\text{\AA}$ )	$k_{eff}$ ( $\text{eV}\text{\AA}^{-2}$ )	$k_3$ ( $\text{eV}\text{\AA}^{-3}$ )	$\omega_D$ ( $\times 10^{13}\text{Hz}$ )
Zn	ACD model	65.377 <sup>b</sup>	0.1698 <sup>c</sup>	1.7054 <sup>c</sup>	2.7931 <sup>c</sup>	2.3887 <sup>a</sup>	1.0528 <sup>a</sup>	3.7552 <sup>a</sup>
	ACE model	65.377 <sup>b</sup>	0.1698 <sup>c</sup>	1.7054 <sup>c</sup>	2.7931 <sup>c</sup>	2.4692 <sup>d</sup>	1.0528 <sup>d</sup>	3.8066 <sup>d</sup>
	Experiment		0.1685 <sup>d</sup>	1.7000 <sup>d</sup>	2.7650 <sup>d</sup>	2.4348 <sup>d</sup>	1.0348 <sup>d</sup>	3.7801 <sup>d</sup>
Cu	ACD model	63,546 <sup>b</sup>	0.3429 <sup>c</sup>	1.3588 <sup>c</sup>	2.8860 <sup>c</sup>	3.1655 <sup>a</sup>	1.0753 <sup>a</sup>	4.3848 <sup>a</sup>
	ACE model	63,546 <sup>b</sup>	0.3429 <sup>c</sup>	1.3588 <sup>c</sup>	2.8860 <sup>c</sup>	3.1655 <sup>e</sup>	1.0753 <sup>e</sup>	4.3848 <sup>e</sup>
	Experiment		0.3300 <sup>f</sup>	1.3800 <sup>f</sup>		3.2000 <sup>f</sup>	1.3000 <sup>f</sup>	4.4086 <sup>f</sup>

<sup>a</sup>This work, <sup>b</sup>Reference [29], <sup>c</sup>Reference [21], <sup>d</sup>Reference [22], <sup>e</sup>Reference [23, 25], <sup>f</sup>Reference [27]

The dispersion relation  $\omega(q)$  of Zn and Cu in the FB zone is calculated by Eq. (6) and is represented in Fig. 1. It can be shown that the obtained results using the ACD are a symmetric function of a linear chain of q, and its maximum value is  $\omega_D$  at the bounds of the FB zone with  $q = \pm\pi/2$ , as seen in Fig. 2. These characteristics of the dispersion relation  $\omega(q)$  are completely consistent with similar obtained results of other crystals in previous works, such as the crystalline iron (Fe) [15], crystalline molybdenum (Mo) [15], and crystalline wolfram (W) [15], and crystalline germanium (Ge) [16].

The temperature dependence of the first EXAFS cumulant  $\sigma^{(1)}(T)$  of (a) Zn and (b) Cu in a range from 0 to 700 K is represented in Fig. 3, in which the obtained results using the ACD model are calculated by Eq. (7). Herein, the values of Cu are smaller than those of Zn, which is because the local force constants  $k_3$  of these metals are roughly equivalent, but Cu has the effective force constant  $k_{eff}$  larger than those of Zn, and this cumulant decreases rapidly as the effective force constant increases, as seen in Table 1. It can be seen that the obtained results using the ACD model are in good agreement with those obtained using the ACE [11-12] model and experiments [11-12, 26, 28]. Also, in comparison with the experimental values, the obtained results using ACD are better in agreement with those obtained using the ACE model, especially in the LT region. For example, the obtained results of Zn using the ACD model, ACE model, and an experiment at  $T \approx 77$  K are  $\sigma^{(1)} \approx 5.29 \times 10^{-3} \text{ \AA}$ ,  $\sigma^{(1)} \approx 5.34 \times 10^{-3} \text{ \AA}$  [11], and  $\sigma^{(1)} \approx 5.26 \times 10^{-3} \text{ \AA}$  [28], respectively. Meanwhile, the obtained results of Cu using the ACD model, ACE model, and an experiment at  $T \approx 80$  K are  $\sigma^{(1)} \approx 3.26 \times 10^{-3} \text{ \AA}$ ,  $\sigma^{(1)} \approx 3.34 \times 10^{-3} \text{ \AA}$  [12], and  $\sigma^{(1)} \approx 3.00 \times 10^{-3} \text{ \AA}$  [26], respectively. Moreover, both the ACD and ACE [11-12] models show the contribution of quantum effects in the LT region, but the obtained results using the ACE model [11-12] are slightly greater than those obtained using the ACD model. The minor difference lies in that the ACE model [11-12] uses only one effective frequency to describe the atomic thermal vibrations, as depicted in Fig. 3.

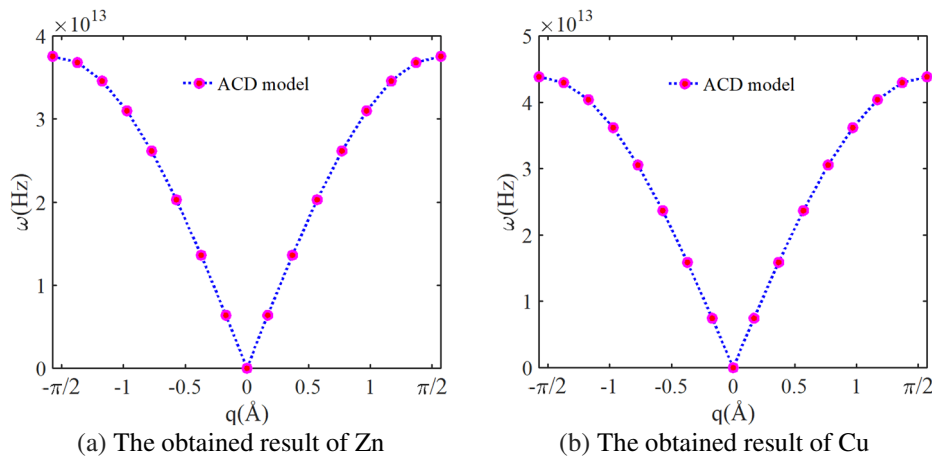


Fig. 2 The dispersion relation of metals obtained from the ACD model

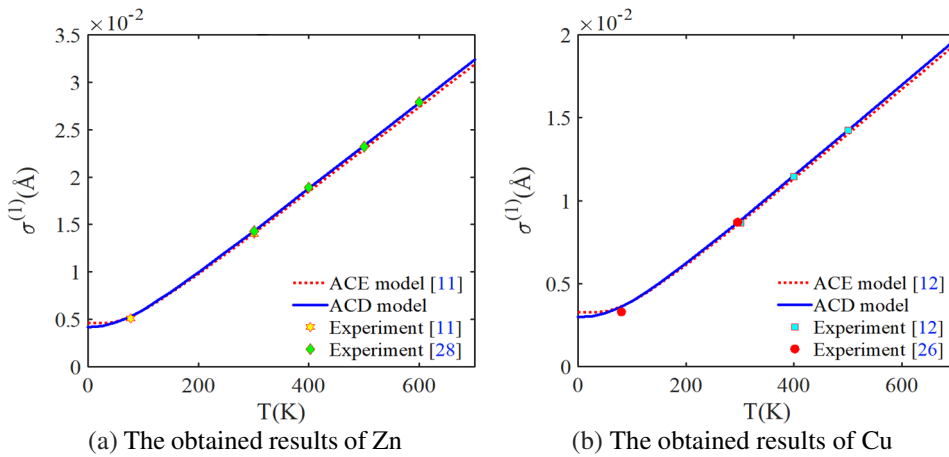


Fig. 3 The temperature-dependent first EXAFS cumulant of metals obtained using the ACD and ACE models and experiments

The temperature dependence of the TE coefficient  $\alpha_T(T)$  of (a) Zn and (b) Cu in a range from 0 to 700 K is represented in Fig. 4, in which the obtained result using the ACD model is calculated by Eq. (8). Herein, the values of Zn are bigger than those of Cu because the temperature-dependent first EXAFS cumulant of Cu changes more slowly than those of Zn, as seen in Fig. 3. It can be seen that the obtained results using the ACD model agree with those obtained using the ACE [11-12] model and

experiments [11-13]. For example, the obtained results of Zn using the ACD model, ACE model, and an experiment at  $T \approx 300$  K are  $\alpha_T \approx 1.57 \times 10^{-5} \text{K}^{-1}$ ,  $\alpha_T \approx 1.56 \times 10^{-5} \text{K}^{-1}$  [11], and  $\alpha_T \approx 1.58 \times 10^{-5} \text{K}^{-1}$  [11], respectively. Meanwhile, the obtained results of Cu using the ACD model, ACE model, and an experiment at  $T \approx 100$  K are  $\alpha_T \approx 0.76 \times 10^{-5} \text{K}^{-1}$ ,  $\alpha_T \approx 0.71 \times 10^{-5} \text{K}^{-1}$  [12], and  $\alpha_T \approx 0.80 \times 10^{-5} \text{K}^{-1}$  [13], respectively. The quantum effects in the ACD model [14] can be shown by the obtained results in the LT limit low temperatures. As shown in the temperature range from above 0 K and below about 10 K, the obtained results of the first EXAFS cumulant are a region of an almost unchanged value, while the obtained results of the TE coefficient correspond to a region of values greater than zero. Moreover, the obtained results using the ACD model are not destroyed quickly in the LT limit as those obtained using the ACE model [11-12], which fits perfectly with Eq. (9) and shows that the ACD model can fully describe the quantum effects. Also, the obtained results using the ACD model increase with the rise of temperature  $T$  and approach the constants in the HT limit, which fits perfectly with Eq. (10) and shows that the ACD model can efficiently describe the anharmonic effects, as seen in Fig. 4. These results are consistent with those obtained by using the quantum methods [11-12, 23].

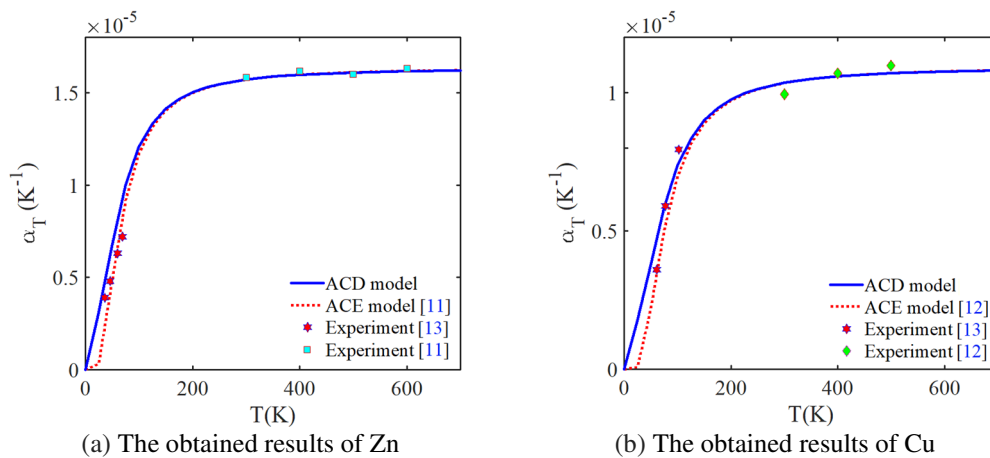


Fig. 4 The temperature-dependent TE coefficient of metals obtained using the ACD and ACE models and experiments

#### 4. Conclusions

In this investigation, the expansion and development of an efficient model have been performed to calculate and analyze the temperature-dependent TE coefficient of metal crystals. The calculated results of the anharmonic TE coefficient using the ACD model satisfied all of their fundamental properties. The TE coefficient increases with increasing temperature  $T$ , which means that the crystal lattice expands strongly at higher temperatures. These results can also describe the influence of anharmonic effects at high temperatures and the influence of the quantum effects at low temperatures on the TE coefficient.

The good agreement of the obtained numerical results for Zn and Cu with those obtained using the ACE model and experiments at various temperatures shows the effectiveness of the present model in investigating the temperature-dependent TE coefficient of metal crystals. This model can be applied to calculate and analyze the anharmonic TE coefficient of other crystals at a temperature ranging from absolute zero degree to their melting points.

#### Acknowledgments

This work is supported by the University of Fire Prevention and Fighting, 243 Khat Duy Tien, Thanh Xuan, Hanoi, Vietnam.

#### Conflicts of Interest

The authors declare no conflict of interest.

## References

- [1] H. Liu, W. Sun, Z. Zhang, L. Lovings, and C. Lind, "Thermal Expansion Behavior in the  $A_2M_3O_{12}$  Family of Materials," *Solids*, vol. 2, no. 1, pp. 87-107, February 2021.
- [2] J. W. Hwang, "Thermal expansion of nickel and iron, and the influence of nitrogen on the lattice parameter of iron at the Curie temperature," Masters Theses, Department of Metallurgical Engineering, University of Missouri–Rolla, Rolla, Missouri, 1972.
- [3] V. A. Drebushchak, "Thermal Expansion of Solids: Review on Theories," *Journal of Thermal Analysis and Calorimetry*, vol. 142, pp. 1097-1113, January 2020.
- [4] T. Dengg, V. Razumovskiy, L. Romaner, G. Kresse, P. Puschnig, and J. Spitaler, "Thermal Expansion Coefficient of WRe Alloys from First Principles," *Physical Review B*, vol. 96, no. 3, pp. 035148, July 2017.
- [5] G. Laplanche, P. Gadaud, O. Horst, F. Otto, G. Eggeler, and E. P. George, "Temperature Dependencies of the Elastic Moduli and Thermal Expansion Coefficient of an Equiatomic, Single-Phase CoCrFeMnNi High-Entropy Alloy," *Journal of Alloys and Compounds*, vol. 623, pp. 348-353, February 2015.
- [6] P. A. Lee, P. H. Citrin, P. Eisenberger, and B. M. Kincaid, "Extended X-Ray Absorption Fine Structure Its Strengths and Limitations as a Structural Tool," *Reviews of Modern Physics*, vol. 53, no. 4, pp. 769-806, October 1981.
- [7] Z. K. Liu, Y. Wang, and S. Shang, "Thermal Expansion Anomaly Regulated by Entropy," *Scientific Reports*, vol. 4, pp. 7043, November 2014.
- [8] Z. K. Liu, Y. Wang, and S. Shang, "Temperature-Dependent EXAFS Debye-Waller Factor of Distorted HCP Crystals," *Journal of the Physical Society of Japan*, vol. 91, no. 5, pp.054703, April 2022.
- [9] T. Yokoyama, K. Kobayashi, T. Ohta, and A. Ugawa, "Anharmonic Interatomic Potentials of Diatomic and Linear Triatomic Molecules Studied by Extended X-Ray Absorption Fine Structure," *Physical Review B*, vol. 53, no. 10, pp. 6111-6122, March 1996.
- [10] T. S. Tien, "Effect of the Non-Ideal Axial Ratio C/A on Anharmonic EXAFS Oscillation of H.C.P. Crystals," *Journal of Synchrotron Radiation*, vol. 28, pp. 1544-1557, September 2021.
- [11] N. V. Hung, C. S. Thang, N. B. Duc, D. Q. Vuong, and T. S. Tien, "Temperature Dependence of Theoretical and Experimental Debye-Waller Factors, Thermal Expansion and XAFS of Metallic Zinc," *Physica B: Condensed Matter*, vol. 521, pp. 198-203, September 2017.
- [12] N. V. Hung, C. S. Thang, N. B. Duc, D. Q. Vuong, and T. S. Tien, "Advances in Theoretical and Experimental XAFS Studies of Thermodynamic Properties, Anharmonic Effects and Structural Determination of FCC Crystals," *The European Physical Journal B*, vol. 90, no.12, pp. 256, December 2017.
- [13] Y. S. Toukian, R. K. Kirby, R. E. Taylor, and P. D. Desai, *Thermophysical Properties of Matter—Thermal Expansion: Metallic Elements and Alloys*, New York: IFI/Plenum, 1975.
- [14] N. V. Hung, N. B. Trung, and B. Kirchner, "Anharmonic Correlated Debye Model Debye-Waller Factors," *Physica B: Condensed Matter*, vol. 405, no. 11, pp. 2519-2525, June 2010.
- [15] N. V. Hung, T. T. Hue, H. D. Khoa, and D. Q. Vuong, "Anharmonic Correlated Debye Model High-Order Expanded Interatomic Effective Potential and Debye-Waller Factors of BCC Crystals," *Physica B: Condensed Matter*, vol. 503, pp. 174-178, December 2016.
- [16] T. S. Tien, "Analysis of EXAFS Oscillation of Monocrystalline Diamond-Semiconductors Using Anharmonic Correlated Debye Model," *European Physical Journal Plus*, vol. 136, no.5, pp. 539, May 2021.
- [17] C. Y. Ho and R. E. Taylor, *Thermal Expansion of Solids*, Ohio: ASM International, 1998.
- [18] J. M. Tranquada, and R. Ingalls, "Extended X-Ray Absorption Fine-Structure Study of Anharmonicity in CuBr," *Physical Review B*, vol. 28, no. 6, pp. 3520-3528, September 1983.
- [19] L. Tröger, T. Yokoyama, D. Arvanitis, T. Lederer, M. Tischer, and K. Baberschke, "Determination of Bond Lengths, Atomic Mean-Square Relative Displacements, and Local Thermal Expansion by Means of Soft-X-Ray Photoabsorption," *Physical Review B*, vol. 49, no. 2, pp. 888-903, January 1994.
- [20] P. M. Morse, "Diatomic Molecules According to the Wave Mechanics. II. Vibrational Levels," *Physical Review*, vol. 34, pp. 57-64, July 1929.
- [21] L. A. Girifalco and V. G. Weizer, "Application of the Morse Potential Function to Cubic Metals," *Physical Review*, vol. 114, no. 3, pp. 687-690, May 1959.
- [22] N. V. Hung, L. H. Hung, T. S. Tien, and R. R. Frahm, "Anharmonic Effective Potential, Effective Local Force Constant and EXAFS of HCP Crystals: Theory and Comparison to Experiment," *International Journal of Modern Physics B*, vol. 22, no. 29, pp. 5155-5166, November 2008.

- [23] N. V. Hung and J. J. Rehr, "Anharmonic Correlated Einstein-Model Debye-Waller Factors," *Physical Review B*, vol. 56, no. 1, pp. 43-46, July 1997.
- [24] T. S. Tien, "Advances in Studies of the Temperature Dependence of the EXAFS Amplitude and Phase of FCC Crystals," *Journal of Physics D: Applied Physics*, vol. 53, no. 31, pp. 315303, June 2020.
- [25] N. V. Hung and P. Fornasini, "Anharmonic Effective Potential, Correlation Effects, and EXAFS Cumulants Calculated from a Morse Interaction Potential for FCC Metals," *Journal of the Physical Society of Japan*, vol. 76, no. 8, article no. 084601, August 2007.
- [26] T. Yokoyama, T. Satsukawa, and T. Ohta, "Anharmonic Interatomic Potentials of Metals and Metal Bromides Determined by EXAFS," *Japanese Journal of Applied Physics*, vol. 28, no. 10R, pp. 1905-1908, October 1989.
- [27] I. V. Pirog, T. I. Nedoseikina, I. A. Zarubin, and A. T. Shuvaev, "Anharmonic Pair Potential Study in Face-Centered-Cubic Structure Metals," *Journal of Physics: Condensed Matter*, vol. 14, no. 8, pp. 1825-1832, February 2002.
- [28] N. V. Hung, T. S. Tien, N. B. Duc, and D. Q. Vuong, "High-Order Expanded XAFS Debye-Waller Factors of HCP Crystals Based on Classical Anharmonic Correlated Einstein Model," *Modern Physics Letters B*, vol. 28, no. 21, pp. 1450174, August 2014.
- [29] J. Meija, T. B. Coplen, M. Berglund, W. A. Brand, P. D. Bièvre, M. Gröning, et al, "Atomic Weights of the Elements 2013 (IUPAC Technical Report)," *Pure and Applied Chemistry*, vol. 88, no. 3, pp. 265-291, February 2016.



Copyright© by the authors. Licensee TAETI, Taiwan. This article is an open access article distributed under the terms and conditions of the Creative Commons Attribution (CC BY-NC) license (<https://creativecommons.org/licenses/by-nc/4.0/>).